Mem. S.A.It. Vol. 94, 141

Memorie della

Radial metallicity gradients of red giant stars in Local Group dwarf galaxies

S. Taibi[1,2,3], G. Battaglia[2,3], R. Leaman[4], A. Brooks[5,6], C. Riggs[5], F. Munshi[7,5,8], Y. Revaz[9], and P. Jablonka[9,10]

[1] Leibniz-Institut für Astrophysik Potsdam (AIP), An der Sternwarte 16, 14482 Potsdam, Germany; e-mail: staibi@aip.de
[2] Instituto de Astrofísica de Canarias, C. Vía Láctea s/n, 38206 La Laguna, Tenerife, Spain
[3] Universidad de La Laguna, Avda. Astrofísico Fco. Sánchez, 38205 La Laguna, Tenerife, Spain
[4] Department of Astrophysics, University of Vienna, Türkenschanzstrasse 17, 1180 Vienna, Austria
[5] Department of Physics & Astronomy, Rutgers, The State University of New Jersey, 136 Frelinghuysen Road, Piscataway, NJ 08854, USA
[6] Center for Computational Astrophysics, Flatiron Institute, 162 Fifth Avenue, New York, NY 10010, USA
[7] Homer L. Dodge Department of Physics & Astronomy, University of Oklahoma, 440 W. Brooks St., Norman, OK 73019, USA
[8] Department of Physics & Astronomy, Vanderbilt University, PMB 401807, Nashville, TN 37206, USA
[9] Institute of Physics, Laboratory of Astrophysics, École Polytechnique Fédérale de Lausanne (EPFL), 1290 Sauverny, Switzerland
[10] GEPI, CNRS UMR 8111, Observatoire de Paris, PSL University, 92125 Meudon, Cedex, France

Received: 28-10-2022; Accepted: 08-11-2022

Abstract. We performed a homogeneous analysis of spectroscopic literature data of red giant stars in 30 dwarf galaxies of the Local Group. We determined their radial metallicity profiles and calculated the associated gradients normalised for the half-light radius, $\nabla_{[Fe/H]}(R/R_e)$. We compared these quantities with several parameters, finding no particular correlations or statistical differences between the inspected dwarf subgroups. We also found that the presence of stellar rotation does not necessarily imply a flat metallicity profile. Instead, the steepest profiles in our sample are observed in systems that probably experienced a dwarf-dwarf merger event in the past. Excluding them, the rest of dwarf galaxies show a distribution of mild gradients with little dispersion. These results agree well with several sets of simulations presented in the literature, analysed using the same method.

Key words. Galaxies: dwarf – galaxies: abundances – techniques: spectroscopic

1. Introduction

The study of the radial metallicity profile of galaxies makes it possible to understand how the interaction between internal dynamics and star formation processes, as well as possible external perturbations, contribute to the spatial distribution of metals within them. In dwarf galaxies, the study of stellar metallicity gradients is more challenging due to their faintness, but no less important. Evidences of stellar metallicity gradients in dwarf galaxies of the Local Group (LG) have been found in both Milky Way (MW) and M31 satellites (e.g. Battaglia et al. 2006, 2011; Ho et al. 2015; Pace et al. 2020), as well as in isolated systems (e.g. Kacharov et al. 2017; Taibi et al. 2018, 2020; Hermosa Muñoz et al. 2020). Only few works have conducted a systematic study in LG systems (Kirby et al. 2011; Leaman et al. 2013), but were limited in their sample of galaxies.

Simulations have shown several mechanisms for the formation of stellar metallicity gradients. For dwarf galaxies evolving in isolation, gradients formation mainly depends on the stellar feedback recipe implemented. For instance, Mercado et al. (2021) showed that recurring and considerable stellar feedback events push old, metal-poor stars outwards with time, leaving young, metal-rich stars concentrated in the centre. On the other hand, in the simulations of Revaz & Jablonka (2018), characterised by low feedback, gradients are formed secularly due to prolonged star formation in the central regions compared to the galaxy outskirts (see also Schroyen et al. 2013, for the role of angular momentum). Past merger events have also been found to produce strong gradients (Benítez-Llambay et al. 2016; Cardona-Barrero et al. 2021), while it is difficult to understand from simulations the role of the environment in shaping the metallicity profile of satellite systems (e.g. Sales et al. 2010, but also Hausammann et al. 2019).

We present here an homogeneous analysis aimed at exploring the radial variation of [Fe/H] measurements in LG dwarf galaxies, as well as to search for correlations with their physical properties. This work is based on results originally published in Taibi et al. (2022).

Table 1. Dwarf galaxy sample and derived parameters. Adapted from Taibi et al. (2022).

Galaxy	$[Fe/H]_0$ [dex]	$\nabla_{[Fe/H]}(R/R_e)$ [dex R_e^{-1}]
SMC	−0.94	−0.101 ± 0.006
Fornax	−0.92	−0.23 ± 0.02
LeoI	−1.32	−0.09 ± 0.01
Sculptor	−1.58	−0.14 ± 0.01
LeoII	−1.53	−0.21 ± 0.03
Carina	−1.69	−0.04 ± 0.03
Sextans	−2.02	−0.32 ± 0.05
Antlia II	−1.75	−0.15 ± 0.07
Ursa Minor	−2.02	−0.15 ± 0.02
Draco	−1.86	−0.07 ± 0.01
Canes Venatici I	−1.91	0.00 ± 0.09
Crater II	−2.16	0.00 ± 0.09
M32	−1.19	0.00 ± 0.05
NGC 205	−0.85	0.00 ± 0.02
NGC 185	−0.44	−0.20 ± 0.03
NGC 147	−0.54	0.00 ± 0.07
Andromeda VII	−1.26	0.00 ± 0.14
Andromeda II	−0.77	−0.39 ± 0.07
Andromeda V	−1.79	−0.10 ± 0.05
NGC 6822	−0.89	−0.46 ± 0.13
IC 1613	−1.10	−0.06 ± 0.08
WLM	−1.27	0.00 ± 0.05
VV 124	−1.25	−0.12 ± 0.04
LeoA	−1.39	−0.16 ± 0.05
Pegasus DIG	−1.21	−0.29 ± 0.12
Sagittarius DIG	−1.84	0.00 ± 0.08
Cetus	−1.55	−0.10 ± 0.05
Aquarius	−1.53	−0.08 ± 0.08
Phoenix	−0.98	−0.35 ± 0.05
Tucana	−1.56	−0.07 ± 0.04

2. Dwarf galaxy sample

We analysed a set of 30 LG dwarf galaxies using publicly available catalogues with spectroscopic metallicity ([Fe/H]) measurements. We selected systems with $\gtrsim$ 50 identified stars, mainly belonging to the red giant branch. The dwarf galaxies we analysed were selected from the satellites of the MW[1] and M31, as well as from those found in isolation. The complete list of systems is given in Table 1, while we refer to Taibi et al. (2022) for the list of refer-

[1] *Excluding the LMC, but also the tidally disrupted Sagittarius dSph (see Vitali et al. 2022, for details on its [Fe/H] gradient).*

ences of the spectroscopic sources and of the adopted parameters. We also refer to the same source for further details on the selection of probable member stars and for the consistency checks performed on the heterogeneous metallicity measurements between catalogues. Here we simply note that the differences between the different methods of determining [Fe/H] were found to have minimal impact on the radial [Fe/H] distribution in our systems.

We examined the [Fe/H] spatial variation in our systems looking for the presence of radial gradients and exploring possible correlations with physical parameters, such as the galaxy stellar mass, the global age of the stellar population, and the galaxy environment. We applied a Gaussian process regression (GPR) analysis method (Pedregosa et al. 2011) in order to follow the radial [Fe/H] variation of a galaxy. Using the GPR, we were able to find the general radial trend in the data while being robust to outliers with no need to choose a functional form a priori. The GPR is in fact a non-parametric Bayesian method that find the radial correlation in the metallicity distribution of our systems by assuming a covariance kernel. The outcome is a smoothed posterior probability distribution of [Fe/H] values as a function of radius, with associated errors.

Figure 1 shows the calculated GPR curves as a function of the radial distance normalised by the galaxy 2D half-light radius R_e. Profiles are either flat or decline with radius, while a slight increase is often seen in the outskirts, which is due to over-fitting of the sparse outer bins and can therefore be neglected. To calculate a system [Fe/H] gradient, we performed a linear fit on the smooth GPR curve between its initial point and the minimum (or the last measured point, in its absence), and took the slope of the linear fit as the gradient's value. The associated error is that of the slope parameter obtained by performing a linear fit to the data instead. The gradients distribution has a median value of $\nabla_{[\mathrm{Fe/H}]}(R/R_e) \sim -0.1$ dex R_e^{-1}, and a median absolute deviation scatter of 0.14 dex R_e^{-1}. Calculated gradient values are reported in Table 1. *Further details on the gradient calculation method (and caveats), with

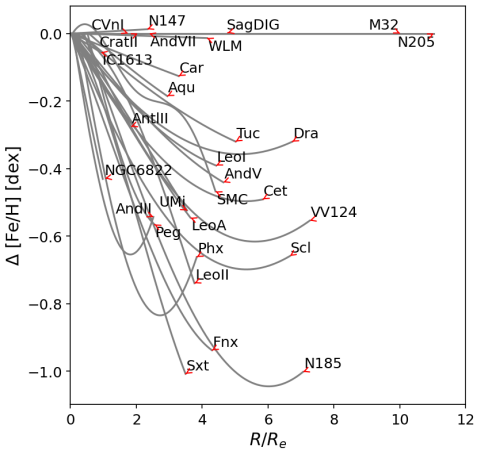

Fig. 1. Smoothed [Fe/H] profiles as obtained from the GPR fitting method as a function of the elliptical radius normalised by the half-light radius. The radial metallicity profiles have been normalised to their value at $R = 0$. Adapted from Taibi et al. (2022).

results on their analysis when expressed in dex kpc^{-1}, are given in Taibi et al. (2022).*

3. Comparison of the stellar metallicity gradients

We compared the calculated metallicity gradients for our sample of dwarf galaxies with several observed quantities, such as morphological type and host distance, stellar mass and star formation timescales. We also investigated the role of angular momentum and past mergers in driving the formation of metallicity gradients.

In Fig. 2 we show the radial [Fe/H] profiles divided according to the morphological type (dE-dSph vs dTr-dIrr), together with the calculated gradients $\nabla_{[\mathrm{Fe/H}]}(R/R_e)$ as a function of distance from the nearest large LG spiral (i.e. MW or M31), colour-coded according to their HI content. In the first case, there is no clear distinction between gas-poor and gas-rich systems, in contrast to the results reported by Leaman et al. (2013), according to which gas-rich systems would present a flat profile, while gas-poor systems would have radially decreasing profiles. This discrepancy can be attributed to the limited *galaxy* sample Leaman et al. analysed. In the second case we confirm our

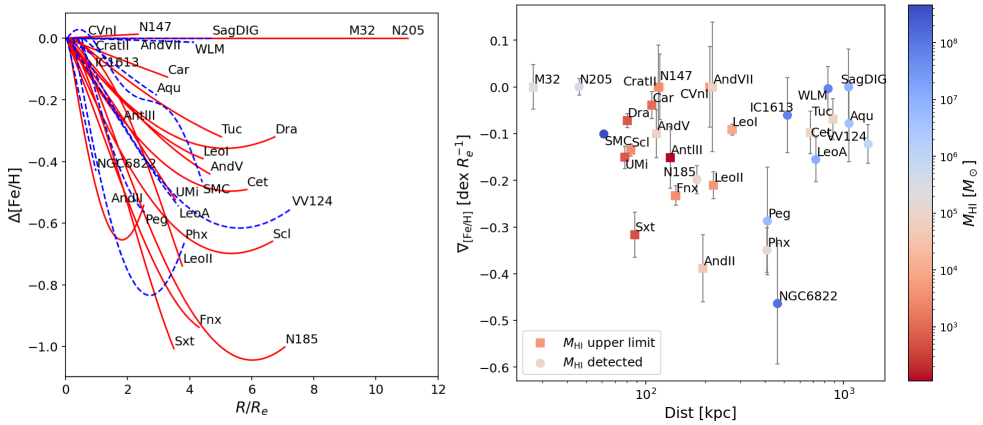

Fig. 2. *Left:* radial [Fe/H] profiles subdivided according to the morphological type of galaxies, where red solid lines indicate gas-poor systems (dE-dSph), while blue dashed lines are for gas-rich systems (dTr-dIrr). *Right:* metallicity gradients as a function of distance from the nearest large LG spiral, with data colour-coded according to their HI content; circles mark a full detection, while squares mark the 5-σ upper limit. Adapted from Taibi et al. (2022).

finding, showing that isolated systems (preferentially gas-rich) have a $\nabla_{[Fe/H]}(R/R_e)$ distribution which is not significantly different from that of the satellite systems (mainly gas-poor). Overall, these two results indicate that the environment (in the sense of prolonged interaction with a host galaxy), which may have played a role in producing the observed morphology-density relation (i.e. in the LG, gas-rich systems are preferentially located further away from the large spirals), did not significantly affected the radial [Fe/H] profiles of the considered dwarf galaxies. We also inspected for any dependencies between the calculated $\nabla_{[Fe/H]}(R/R_e)$ and the galaxy luminosity in the V-band or the galaxy star formation history (SFH) duration. In both cases, we did not find any significant dependence.

Finally, in Fig. 3 we explore the contribution of angular momentum in flattening the radial [Fe/H] profiles (*left* panel), and the possible association with past mergers for those systems showing the steepest profiles (*right* panel). Concerning the first point, simulations have shown that in a dwarf galaxy evolving with a rotationally supported disk of gas, star formation cannot effectively funnel towards the centre, thus preventing the formation of a radial [Fe/H] gradient (Schroyen et al. 2013). This effect should be stronger in dwarf galaxies with high stellar masses and a prolonged SFH (Revaz & Jablonka 2018). In our sample, significant stellar rotation (i.e. with $0.5 \lesssim V_{rot}/\sigma_v \lesssim 2.0$) has been detected in 12 systems (highlighted in blue in Fig. 3, left). Selecting those dwarf galaxies with high stellar masses and extended SFHs (7 systems with $\log(L_V/L_\odot) > 7.5$ and $\log(t_{90}/yr) < 9.6$) three show declining profiles (one, NGC 6822, could however be associated with a past merger, see below), while the others are rather flat within errors. The same cannot be said for the rotating systems of lower mass, which show a variety of decreasing profiles (although again two systems with the steepest profiles, And II and Phoenix, may have undergone a past merger). Therefore, it is difficult to recover a clear contribution of angular momentum.

Regarding the second point instead, we have found that those systems showing evidences of a past ($z \lesssim 1$) major merger, all have steep declining profiles (or $\nabla_{[Fe/H]}(R/R_e) < -0.25$ dex R_e^{-1}, see Fig. 3, right). This is in agreement with simulations showing how a past merger could lead to the formation of a strong [Fe/H] gradient (Benítez-Llambay et al. 2016; Cardona-Barrero et al. 2021). We refer to Taibi et al. (2022), for further details.

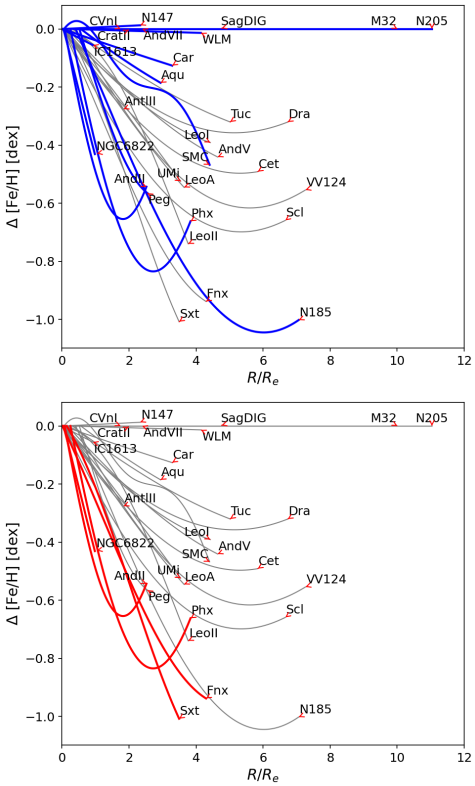

Fig. 3. Radial [Fe/H] profiles colour-coded according to whether a dwarf galaxy shows stellar rotation (blue lines, *left* panel) or has been associated with a past merger event (red lines, *right* panel). Figures reproduced using data from Taibi et al. (2022).

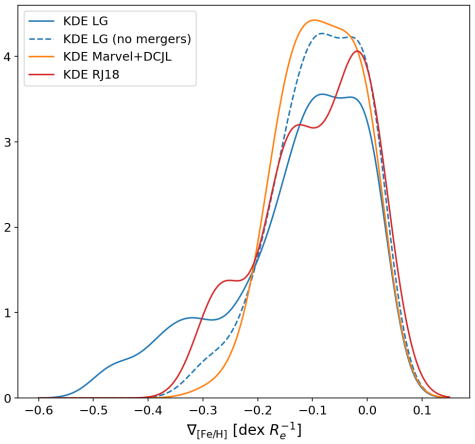

Fig. 4. Kernel density estimation (KDE) of the metallicity gradient distribution for the observed sample (with and without merger candidates as solid and dashed blue lines, respectively), compared with the simulated sets of Revaz & Jablonka (2018, red line) and the MARVEL plus DCJL ones (orange line). Adapted from Taibi et al. (2022).

3.1. Comparison with simulations

We compared our results with three different set of simulations from the literature that specifically inspected the formation of metallicity gradients in dwarf galaxies. Namely, we compared with simulations from Mercado et al. (2021), Revaz & Jablonka (2018), and those presented in Bellovary et al. (2019), Akins et al. (2021) and Munshi et al. (2021), also known as MARVEL and DCJL. They cover a similar luminosity range as the observations, but were generated using distinct hydrodynamic codes and stellar feedback recipes.

The comparison with Mercado et al. (2021) concerned the possibility of reproducing their prediction of a strong correlation between [Fe/H] gradients and the galaxy median ages, namely that older galaxies should have steeper [Fe/H] profiles. We performed the comparison using their tabulated values, making sure that we obtained our gradients following their own method. Thanks to our large sample (larger than the one they considered), we found that the observed correlation is very mild and does not seem to support their prediction.

With the other sets of simulations, we were instead able to directly apply our analysis method on the simulated data, performing an homogeneous comparison with the observations. Our results are summarised in Fig.4. It can be appreciated that the simulated systems have gradient distributions comparable to those observed, particularly when excluding observed systems probably associated with a past merger. Despite this obvious success, it is difficult to explain why simulated systems do not show such strong [Fe/H] gradients as those observed, since dwarf-dwarf mergers are naturally included in the considered simulations. It is true that this discrepancy could be mitigated by taking into account the associated errors in both observations and simulations, which

would leave a discrepancy only with the simulated MARVEL and DCJL sets. It should also be noted that this is a first attempt to directly compare high-resolution simulations with observations, and further inspections are needed to fully recover the sources of the discrepancy. See Taibi et al. (2022) for further details.

4. Conclusions

We conducted an homogeneous analysis of stellar metallicity gradients in a selected sample of LG dwarf galaxies using publicly available spectroscopic data. This is the largest compilation of this type to date.

We examined the radial [Fe/H] profiles of our systems by applying a Gaussian process regression analysis, from which we were able to derive the [Fe/H] gradients. We compared these values with several observed quantities for our systems, such as morphological type, host distance, luminosity, star formation history, stellar rotation and past merger history. In all cases, we did not find a clear driver of [Fe/H] gradient formation, except for those systems associated with a past dwarf-dwarf merger event, which show the steepest radial [Fe/H] profiles. Excluding such merger candidates, the observed systems show similarly mild gradients within a small dispersion, regardless of stellar mass, SFH or environment, indicating that their formation is an intrinsic aspect of the evolution of dwarf galaxies.

Direct comparison with different sets of simulations has also not allowed us to firmly establish the preferred formation mechanism of the [Fe/H] gradients. However, we could exclude an inside-out scenario driven by strong stellar feedback events, such as the one simulated in Mercado et al. (2021). Instead, it appears that a combination of stellar migration due to feedback events and efficient central star formation may concur in producing the observed gradient's distribution. To further inspect this aspect, stellar ages should also be taken into account if a meaningful age-metallicity relationship can be provided for each of our systems.

Acknowledgements. ST is grateful for the referee's helpful comments and to the organisers of the "Hack100" conference (Trieste, 6-10 June 2022) for the opportunity to give a talk on this work.

References

Akins, H. B., Christensen, C. R., Brooks, A. M., et al. 2021, ApJ, 909, 139
Battaglia, G., Tolstoy, E., Helmi, A., et al. 2011, MNRAS, 411, 1013
Battaglia, G., Tolstoy, E., Helmi, A., et al. 2006, A&A, 459, 423
Bellovary, J. M., Cleary, C. E., Munshi, F., et al. 2019, MNRAS, 482, 2913
Benítez-Llambay, A., Navarro, J. F., Abadi, M. G., et al. 2016, MNRAS, 456, 1185
Cardona-Barrero, S., Battaglia, G., Di Cintio, A., Revaz, Y., & Jablonka, P. 2021, MNRAS, 505, L100
Hausammann, L., Revaz, Y., & Jablonka, P. 2019, A&A, 624, A11
Hermosa Muñoz, L., Taibi, S., Battaglia, G., et al. 2020, A&A, 634, A10
Ho, N., Geha, M., Tollerud, E. J., et al. 2015, ApJ, 798, 77
Kacharov, N., Battaglia, G., Rejkuba, M., et al. 2017, MNRAS, 466, 2006
Kirby, E. N., Lanfranchi, G. A., Simon, J. D., Cohen, J. G., & Guhathakurta, P. 2011, ApJ, 727, 78
Leaman, R., Venn, K. A., Brooks, A. M., et al. 2013, ApJ, 767, 131
Mercado, F. J., Bullock, J. S., Boylan-Kolchin, M., et al. 2021, MNRAS, 501, 5121
Munshi, F., Brooks, A. M., Applebaum, E., et al. 2021, ApJ, 923, 35
Pace, A. B., Kaplinghat, M., Kirby, E., et al. 2020, MNRAS, 495, 3022
Pedregosa, F., Varoquaux, G., Gramfort, A., et al. 2011, Journal of Machine Learning Research, 12, 2825
Revaz, Y. & Jablonka, P. 2018, A&A, 616, A96
Sales, L. V., Helmi, A., & Battaglia, G. 2010, Advances in Astronomy, 2010, 194345
Schroyen, J., De Rijcke, S., Koleva, M., Cloet-Osselaer, A., & Vandenbroucke, B. 2013, MNRAS, 434, 888
Taibi, S., Battaglia, G., Kacharov, N., et al. 2018, A&A, 618, A122
Taibi, S., Battaglia, G., Leaman, R., et al. 2022, A&A, 665, A92
Taibi, S., Battaglia, G., Rejkuba, M., et al. 2020, A&A, 635, A152
Vitali, S., Arentsen, A., Starkenburg, E., et al. 2022, MNRAS, -,